

# A Nano-Joule Burst-Mode Eye-Gaze Angle and Object Distance Sensor for Smart Contact Lenses

Chayanjit Ghosh, Sakthidasan Kalidasan, Mohit U. Karkhanis, Alex Mastrangelo, Aishwaryadev Banerjee, Ross Walker, Hanseup Kim and Carlos H. Mastrangelo

ECE Department, University of Utah, Salt Lake City, USA

[chayanjit@gmail.com](mailto:chayanjit@gmail.com)

**Abstract**—In this article, we demonstrate an ultra-low energy eye gaze tracking system and distance ranger based on scleral coils developed specifically for smart contact lenses. The system comprises of a set of four (two transmitter and two receiver) semi-circular, copper coils which are patterned on flexible Kapton substrates conformally placed on the eye scleras. The thickness of the entire assembly is  $\sim 100\ \mu\text{m}$ . A high-frequency amplitude modulated AC signal is transmitted from a transmitter coil in short bursts, which induces an EMF in a receiver coil that is a function of the eye-gaze angle. The induced voltage is demodulated using an AM receiver IC. The observed object distance from the eyeballs can be determined via triangulation of the measured eye-gaze angles. Preliminary results demonstrate that a very short burst of transmitted signal  $31\ \mu\text{s}$  long is sufficient for peak envelope detection of the received signal, requiring only  $340\ \text{nJ}$  of total energy per distance range measurement. This is about  $1/500,000$  of the energy per measurement required by miniature solid-state time-of-flight distance sensors.

**Keywords**— distance-sensor; eye-tracking; scleral coils; low-power; smart contact lens

## I. INTRODUCTION

Presbyopia is the physiological inability of an aging eye to focus clearly on objects located at different distances from the eye, which leads to loss of image focus, blurry vision and visual impairment. Worldwide, more than 1.8 billion people are plagued by this condition of accommodation deficiency [1], [2]. Therefore, techniques for presbyopia-correction have been widely pursued, and mostly include fixed corrective (bifocal, multifocal and progressive) lenses. However, a more useful approach is to use adaptive eyeglasses or smart contact lenses, that can automatically change the optical power of the contact lens depending on the distance and location of the object of focus, thereby producing a sharp image of the object in the field of vision [3]–[10]. For practical realization of such a system, it is necessary to use an eye-tracker that can accurately determine the vergence angle of the observer eyes and the distance of the object of interest from the observer. Furthermore, since a standalone smart contact lens system has access to limited electrical energy [11], it is also imperative that the eye-tracker consumes significantly low energy for reliable operation. Therefore, low-power, passive techniques which utilize scleral coils to determine the eye gaze angles, and by extension the object distance, are more desirable for such purposes.

Recently, we demonstrated a method that utilizes angle-dependent electromagnetic induction from one set of drive coils on one eye to a receiver coil on other eye to determine the relative angle between the two eyes thereby eliminating the requirement of power-hungry, external AC-driven

electromagnets, which are utilized in traditional scleral coil-based eye trackers. However, for successful integration with a smart contact lens platform, one must carefully design the eye-tracking system to operate reliably, while using very-low amounts of energy per angle measurement.

In this article, we present a novel, ultra-low energy implementation of a scleral coil-based eye-gaze angle sensor, where four coils (two transmitters and two receivers) are placed on the sclera, two per eyeball. In our technique, we transmit a high-frequency amplitude modulated AC signal from the transmitter coil, which induces a gaze-angle dependent EMF in the receiver coil, which is demodulated using a commercially available AM radio receiver IC and the induced peak voltage is recovered. As detected by the IC, a significantly short demodulation time allows for peak-detection of the induced EMF, utilizing only very short bursts of transmitted signals using extremely low energy which is ideal for integration with a standalone smart contact lens system.

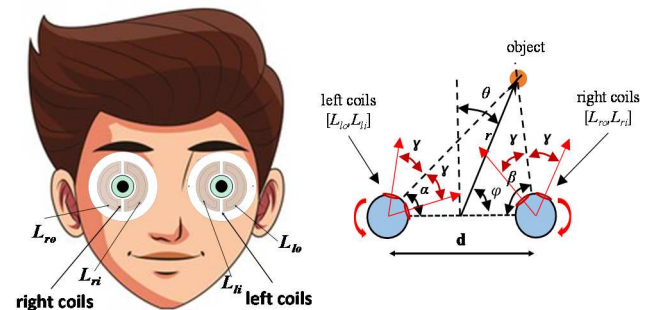


Fig. 1. Working principle of scleral coil based eye-gaze angle sensor. Working principle of scleral coil based eye-gaze angle and object distance sensor.

## II. WORKING PRINCIPLE

Fig. 1 shows a schematic of the working principle of the quad-coil range detector. Two flexible semi-circular scleral coils are placed on the eye-ball. Taking the midpoint between the eyes as a reference-point, these coils are identified as either inner or outer and are suitably labelled as vector  $[L_{lo}, L_{li}, L_{ri}, L_{ro}]$ . Both coils on a single eyeball (transmitter coil) are connected to an AC signal generator that supplies the transmitter coil with an amplitude modulated, high-frequency signal. The electromagnetic field generated by these coils interfere constructively and induce an electromotive force (EMF) on the other pair of scleral coils (receiver coils) that are placed on the other eyeball. A commercially available AM radio receiver IC detects the induced signal and demodulates it to recover the peak induced voltage, which is a function of the relative angle

between the two coils. While the angle between the coils placed on the same eyeball is constant, that between the transmitter and receiver coils varies when an observer steers towards an object of interest. The detected peak induced voltage is dependent on the eye-gaze angles  $\alpha$  and  $\beta$ , to uniquely determine the distance and direction of the object of interest according to Eq. (1). Therefore, the steering angles and the object distance ( $r$ ), can be accurately calculated using triangulation techniques as shown in Fig. 1. Angles  $\theta_L$  and  $\theta_R$  are the left and right eyeball gaze angles, where  $\theta_L = \pi/2 - \alpha$  and  $\theta_R = \beta - \pi/2$  and the object bearing angle  $\theta = (\theta_L + \theta_R)/2$ . The vergence angle is  $\theta_V = (\theta_R - \theta_L)$ .

$$r = \frac{d}{(\cot(\alpha) + \cot(\beta))} \quad (1)$$

#### A. Equivalent Electrical Model

The equivalent electrical circuit of the bearing-angle sensor is a transformer, where the coefficient of mutual inductance is  $M$ , is a function of the eye-steering angles  $\alpha$  and  $\beta$ . Since the diameter of the scleral coils is significantly smaller than the distance between the coils, the closed form solution of the of the bearing-angle dependent mutual inductance can be approximated by Eq. (2).

$$M(\alpha, \beta) \approx \frac{\mu_o}{4\pi} \cdot A_s A_r N_s N_r \frac{[3 \cdot \hat{r}(\hat{r} \cdot \hat{n}_s) - \hat{n}_s] \cdot \hat{n}_r}{\|\hat{r}\|^3} \quad (2)$$

Where  $\mu_o$  is the vacuum permeability,  $A_s$  and  $A_r$  are the areas of the source and receive coils respectively,  $N_s$  and  $N_r$  are the number of turns of the source and receive coils respectively,  $\hat{r}$  is the vector from the center of the source coil to the center of the receive coil,  $\hat{r}$  is the same normalized vector and  $\hat{n}_s$  and  $\hat{n}_r$  are the normals to the source and receive coils respectively.

#### B. Minimizing Operating Energy Requirements using Burst Transmission

For minimizing the energy required to measure the eye-gaze angles, one must suitably minimize the duration of the transmitted signal burst. The minimum burst duration is given by the settling time required for the demodulated signal to reach a steady-state peak-value. This is determined by several factors which include the quality factor at the driving frequency and the envelope detector configuration.

### III. COIL DESIGN AND FABRICATION

For maximizing the induced EMF, (a) the mutual inductance to self-inductance ratio ( $M_{s,r}/L_s$ ) and (b) the coil resistance  $R$  need to be optimized. For a given coil surface area, the ratio of the mutual to self-inductance can be maximized by maximizing the number of coil turns. However, this also results in a higher coil resistance, which undesirably reduces the final peak value of induced EMF. Alternatively, one can increase the thickness of the metallic wires which form the coils. Additionally, for successfully integrating the eye-tracker system with a smart contact lens platform, the coils need to be fabricated on a flexible substrate and the system needs to be suitably engineered to prevent fracture or breaking of the metallic lines upon necessary deformation when mounting them on similar non-planar surfaces.

The coils were custom-built (PCBway) on a  $\sim 100 \mu\text{m}$ -thick, flexible PCB Kapton substrate and each coil was designed to feature 5 turns. The inner radius was 6 mm and

the outer radius is 10 mm. The coils were fabricated using Cu wires which were  $\sim 55 \mu\text{m}$  thick. Electrical measurements revealed that the resistance of the coil was  $\sim 2.5 \Omega$  and the inductance was  $\sim 2000 \text{ nH}$ . Fig. 2 shows an optical image of the flexible scleral coils. Two of these coils were mounted on a 25.4 mm diameter rubber balls as shown in the figure below. The resulting coil mount was wrinkle-free, thereby demonstrating good conformality.



Fig. 2. Optical images of a pair fabricated scleral coil (left) and coil mounted on polymeric sphere (right).

## IV. EXPERIMENTS AND RESULTS

#### A. Experimental Setup

The flexible coils were conformally placed on polymeric spheres of 25 mm diameter, placed 60 mm apart, which closely resembles the dimensions and position of eyeballs on a typical human face. A signal generator (Siglent SDG 2082x) was connected to the left inner transmitter coils for providing an amplitude modulated high-frequency AC signal. The right inner receiver coil was connected to a single chip AM radio receiver IC (TA7642) which features in-built automatic gain control (AGC) to detect the peak induced EMF at the receiver coil. AGC is a closed-loop feedback mechanism which detects the overall strength of the received signal and automatically adjusts the gain of the receiver IC, thus enabling detection of received signals as weak as  $600 \mu\text{V}$ . The receiver chip demodulates the induced EMF and performs envelope detection of the received signal, thereby producing stable, angle-dependent DC voltages that are measured for determining the eye-gaze angles. This detection circuit consumes a quiescent current of  $200 \mu\text{A}$  and has a footprint of  $24.35 \text{ mm}^2$  excluding the receiver coil.

The output of the AM receiver chip was probed using a RIGOL DS 1074 oscilloscope to measure the recovered peak voltage. To obtain the maximum induced EMF, the frequency of the AC signal was maintained at the resonant frequency of the system, which was experimentally determined prior to data collection by using Siglent SSA 3021X spectrum analyzer. To record the peak induced EMF at various steering angles, the polymeric spheres were mounted on a long PTFE shaft that was driven by two high-resolution stepper motor (Hitec D950 TW), which was controlled by an automated Python script. Peak detected voltages were recorded at gaze angles from  $-30^\circ$  to  $+30^\circ$  at an interval of  $10^\circ$ .

Fig. 3 shows the schematic of the experimental setup and the entire circuit diagram of bearing-angle sensor, respectively. The plastic TO-92 package of the TA7642 chip can be thinned down using appropriate techniques, enabling its integration onto a low-profile contact lens platform.

#### B. Frequency Response

To determine the coil system resonant frequency, which produces maximum induction at the receiver coil, the left inner transmitter coil was connected to the signal generator

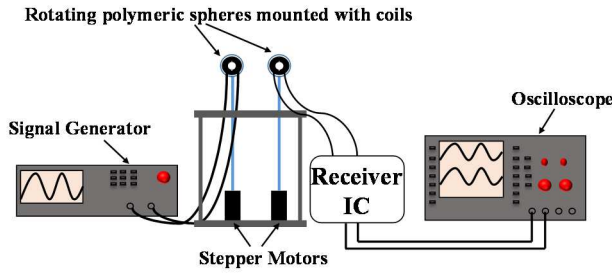


Fig. 3. Experimental setup for measuring eye-gaze angle dependent induced EMFs.

and the right inner receiving coil was probed using a spectrum analyzer. The measured capacitance of the coaxial lines used for electrical interconnects was 150 pF and the instrument resistance was  $\sim 50 \Omega$ . The transfer function amplitude measurements ( $\|V_r/V_g\|$ ) revealed a sharp resonance peak at  $\sim 2.5$  MHz with a maximum gain of -37 dB. Therefore, all subsequent measurements were performed at a resonant frequency of 2.5 MHz.

### C. Angular Response at Resonance

The induced EMF at the receiver coil was measured at resonance, for different gaze angles, from  $-30^\circ$  to  $30^\circ$ . The inner coil of the left eyeball was the transmitter coil, and was provided with an amplitude modulated input signal of  $5 V_{p-p}$  at a frequency of 2.5 MHz and the inner coil of the other eyeball was the receiver coil, which was connected to the AM receiver IC chip, that was probed with an oscilloscope. Fig. 4 shows the induced peak-voltage as detected by the receiver chip at resonance as a function of eyeball gaze-angles  $[\theta_L, \theta_R]$ . The resultant plot has a broad peak configuration symmetric around the  $\theta_L = -\theta_R$  corresponding to the two eyeballs converging to a point straight in front of the midpoint. Therefore, reliable detection of the peak induced voltage allows for accurate estimation of the eyeball gaze angle and by extension, the bearing angle. The method to get the bearing angle and range distance from this data is discussed in [12].

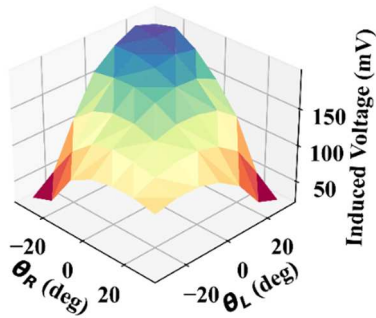


Fig. 4. Induced RMS voltage recorded at resonance at the receive coils versus eye ball gaze angles

### D. Settling-Time Measurements and Energy Requirements

In order to minimize the energy required for peak detection of the induced EMF, one can simply transmit bursts of high-frequency AC signals from the transmitter coil, instead of a continuous transmission as demonstrated previously [12]. However, for reliable detection, one must ensure that the duration of the burst-mode signal, or pulse-width is sufficiently wide for the receiver chip to detect the peak value of the induced EMF. To determine the minimum pulse-width

of the transmitted signal, we measured the time required for the detected EMF to reach its peak-value, also known as the settling time. If the burst duration is any shorter than the detector settling time, the receiver chip is unable to detect the peak of the induced EMF and the eye-tracker system is unable to provide correct information regarding the eye-gaze angle.

As shown in Fig. 5, oscilloscope measurements revealed that the settling-time for the system was  $\sim 31 \mu s$ . Therefore, the minimum pulse-width of the transmitted signal is  $31 \mu s$ . At resonance, the measured real impedance magnitude of the entire system was  $\sim 458 \Omega$ . The output from the signal generator was set to be  $5 V_{p-p}$  but the voltage across the transmitter coils was measured to be  $\sim 4.48 V_{p-p}$ . The calculated instantaneous power consumption was 10.95 mW. Therefore, with a pulse-width of  $31 \mu s$ , the energy consumed for transmitting one burst signal was  $\sim 340$  nJ.

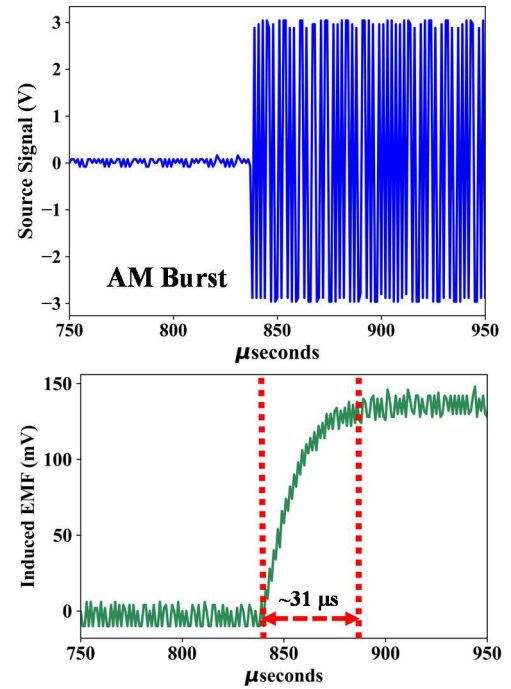


Fig. 5. Transmitted AM AC signal and transient induced EMF detected by the receiver chip.

This energy consumption is two orders of magnitude lower than the eye-tracker system previously presented by the authors, which was operated using a continuously transmitted AC signal [12] and  $1/500,000$  of that required for solid-state time-of-flight distance sensors (VL53L0X, ST Micro).

### SUMMARY

We have developed a burst-mode induction-based eye glaze angle and distance ranger that requires 340 nJ of energy per measurement thus making this system suitable for ultra-low power applications such as extreme power-constrained smart contact lenses.

### ACKNOWLEDGMENT

This work has been supported by the National Science Foundation grant CNS-1932602. The authors would like to thank Erfan Pourshaban and Adwait Deshpande for their help and invaluable suggestions.

## REFERENCES

- [1] T. R. Fricke *et al.*, “Global Prevalence of Presbyopia and Vision Impairment from Uncorrected Presbyopia Systematic Review, Meta-analysis, and Modelling,” *Ophthalmology*, vol. 125, pp. 1492–1499, 2018, doi: 10.1016/j.ophtha.2018.04.013.
- [2] C. H. M. Mohit U. Karkhanis, Aishwaryadev Banerjee, Chayanjit Ghosh, Rugved Likhite, David Meyer, “Models of Accommodation Deficiency in Presbyopia Patients,” *medRxiv*, 2020, doi: <https://doi.org/10.1101/2020.08.12.20173724>.
- [3] N. Padmanaban, R. Konrad, and G. Wetzstein, “Autofocals: Evaluating gaze-contingent eyeglasses for presbyopes,” *Sci. Adv.*, vol. 5, no. 6, Jun. 2019, doi: 10.1126/sciadv.aav6187.
- [4] J. Jarosz *et al.*, “Adaptive eyeglasses for presbyopia correction: an original variable-focus technology,” *Opt. Express*, vol. 27, no. 8, p. 10533, Apr. 2019, doi: 10.1364/oe.27.010533.
- [5] J. Mompeán, J. L. Aragón, and P. Artal, “Portable device for presbyopia correction with optoelectronic lenses driven by pupil response,” *Sci. Rep.*, vol. 10, no. 1, pp. 1–9, Dec. 2020, doi: 10.1038/s41598-020-77465-5.
- [6] M. U. Karkhanis *et al.*, “Correcting Presbyopia with Autofocusing Liquid-Lens Eyeglasses,” Jan. 2021.
- [7] C. Ghosh *et al.*, “Micropower Object Range and Bearing Sensor for Smart Contact Lenses,” in *2020 IEEE SENSORS*, Oct. 2020, pp. 1–4. doi: 10.1109/SENSORS47125.2020.9278622.
- [8] A. Majumder *et al.*, “Creep deformation in elastomeric membranes of liquid-filled tunable-focus lenses,” *Appl. Opt.*, vol. 58, no. 23, p. 6446, Aug. 2019, doi: 10.1364/AO.58.006446.
- [9] N. Hasan *et al.*, “Tunable-focus lens for adaptive eyeglasses,” *Opt. Express*, vol. 25, no. 2, p. 1221, Jan. 2017, doi: 10.1364/OE.25.001221.
- [10] N. Hasan *et al.*, “A Low-Power Light-Weight Tunable Lens for Ophthalmic Applications,” in *Imaging and Applied Optics 2016*, 2016, p. AOM3C.4. doi: 10.1364/AOMS.2016.AOM3C.4.
- [11] E. Pourshaban *et al.*, “Micromachined Flexible Semi-Transparent Silicon Solar Cells as Power Sources for Microsystems,” in *2021 IEEE 34th International Conference on Micro Electro Mechanical Systems (MEMS)*, Jan. 2021, pp. 246–249. doi: 10.1109/MEMS51782.2021.9375382.
- [12] C. Ghosh *et al.*, “Low-Profile Induced-Voltage Distance Ranger for Smart Contact Lenses,” *IEEE Trans. Biomed. Eng.*, vol. 68, no. 7, pp. 2203–2210, Jul. 2021, doi: 10.1109/TBME.2020.3040161.